Supplementary Material

Impact of surface grafting density of PEG macromolecules on dually fluorescent silica nanoparticles used for the in vivo imaging of subcutaneous tumors.

Laurent Adumeau [a], Coralie Genevois [b], Lydia Roudier [a], Christophe Schatz [c], Franck Couillaud [b], Stéphane Mornet [a]

[a] CNRS, Univ. Bordeaux, ICMCB, UPR 9048, F-33600 Pessac, France.

[b] Univ. Bordeaux, EA 7435 IMOTION - Imagerie moléculaire et thérapies innovantes en oncologie, 33706 Bordeaux, France.

[c] CNRS, Univ. Bordeaux, LCPO, UMR 5629, F-33600, Pessac, France

1. Amino-Functionalized Silica Nanoparticles Characterization.

1.1 Diffuse reflectance IR spectroscopy.

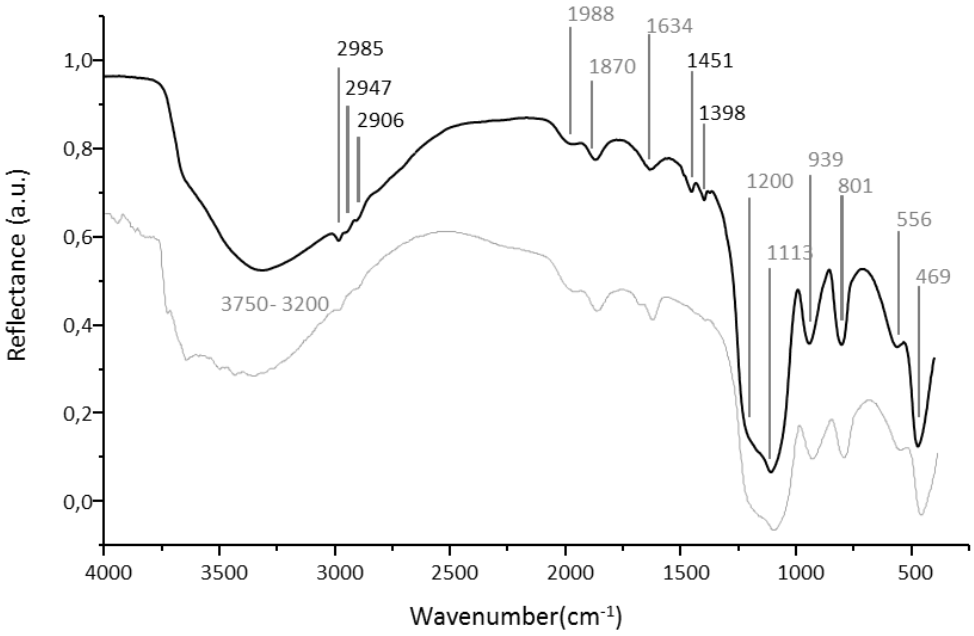

Figure S1. DRIFT spectra of DF-SiO_2 nanoparticles before (grey spectrum) and after (dark spectrum) silanization by EDPS.

DRIFT spectrum of DF-SiO_2NPs is characterized by the presence of typical vibration bands generally observed for colloidal silica prepared b sol-gel method. It can be thus observed the vibration bands from 400-1200 cm^{-1} characterized as Si-O-Si vibration and the bands between 1600-2000 cm^{-1}. The two bands of weak intensity in the range of 2900 to 3000 cm^{-1} can be attributed to vibrations of alkyl chains of remaining ethoxy groups or due to the presence of fluorescent dyes present in few amounts inside the silica matrix. The broad and intense band at 3200 - 3750 cm^{-1} is attributed to the stretching vibrations of hydrogen bonds and Si-OH groups covering the surface of the colloidal silica, H-bonded H_2O and H-bonded OH vibrations of alcohol. The bands in the range of 1600 to 2000 cm^{-1} have also been observed [1]. The band at 1872 cm^{-1} can be identified as a typical silica overtone band [2,3]. It has been supposed that the band at 1630 cm^{-1} is due to H_2O molecules [4] incorporated in the matrix and has been identified as scissor-bending vibration of matrix intercalated molecular water [5]. The vibration bands in the range of 400-1200 cm^{-1} are fully attributed to Si-O-Si vibrations. The band

at 1108 cm^{-1} belongs to antisymmetric stretching vibrations, possessing a shoulder at 1190 cm^{-1}. This shoulder appears due to a splitting of longitudinal optical and transverse optical stretching motions. The band at 938 cm^{-1} has been attributed to Si-O-Si stretching vibrations, the band at 803 cm^{-1} to Si-O-Si bending and the band at 468 cm^{-1} to Si-O-Si rocking vibrations. The weaker band at 561 cm^{-1} arises due to cyclic structures in the silica network [5,6].

DF-SiO_2NPS-EDPS spectrum displays additional bands attesting the presence of the organofunctional polysiloxane film. In addition to the weak bands between 2985 cm^{-1} and 2906 cm^{-1} attributed to asymmetric and symmetric stretching vibrations of C-H bonds, an extra band at 2947 cm^{-1} attributed to C-H stretching vibrations of the methyl groups attached to a nitrogen atom, can be observed. In the range from 1500 to 1300 cm^{-1} we can distinguish two vibration bands, which arise after modification with EDPS. The band at 1451 cm^{-1} is attributed to twisting C-H deformation vibrations and another band of C-N stretching vibrations which arises at a value of 1398 cm^{-1}.

1.2 Zeta potential measurements.

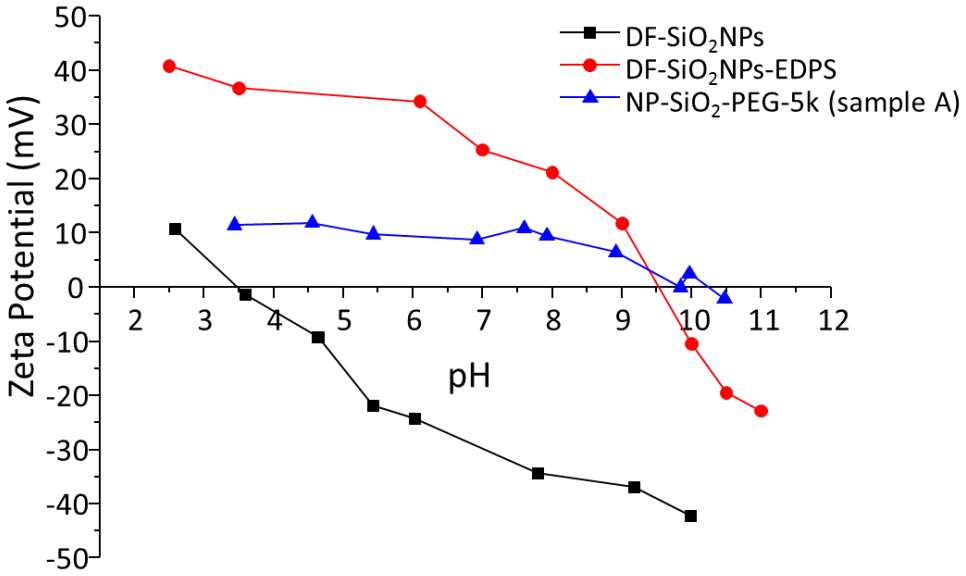

Figure S2. Plots of ζ potential values as a function of pH of bare DF-SiO_2 nanoparticles (■) compared with amino-functionalized DF-SiO_2 nanoparticles (●) and PEGylated DF-SiO_2 nanoparticles (▲, sample A).

Zeta potential values of modified and unmodified silica nanoparticles diluted at a final concentration of 0.1 mg/mL were measured for a pH range (pH = 1-12) in water (medium of weak conductivity $\Lambda \approx 0.1$ mS/cm). The zeta potential curve (Figure S2) of silica nanoparticles displayed an isoelectric point (IEP) at pH 3-3.5, in agreement with previous reports [7]. After silanization of the silica surface, the IEP of aminated nanoparticles reached a pH value of 9.5 that corresponds to the pKa of the primary aminopropyl group. This result indicated a high density of amino groups exposed to the modified-nanoparticle surface [8]. Because of the thermal treatment, the condensation of polysiloxane film is completed on the surface triggering the rupture of intramolecular interactions between silanol and the amino groups [9,10]. Moreover, the presence of these protonable amino groups in neutral pH conditions ensures the electrostatic colloidal stability. In the case of PEGylated NPs, the surface exhibits smaller zeta potential values due to the presence of the polymer corona which directly impacts the ζ values by moving the slipping plane away from the surface. Although values decrease drastically, they remain positive due to the presence of free inner tethering amine sites and by the fact that primary amine groups are converted to secondary amines during the reaction.

2. ^{1}H-NMR spectrum of mPEG5K-ald.

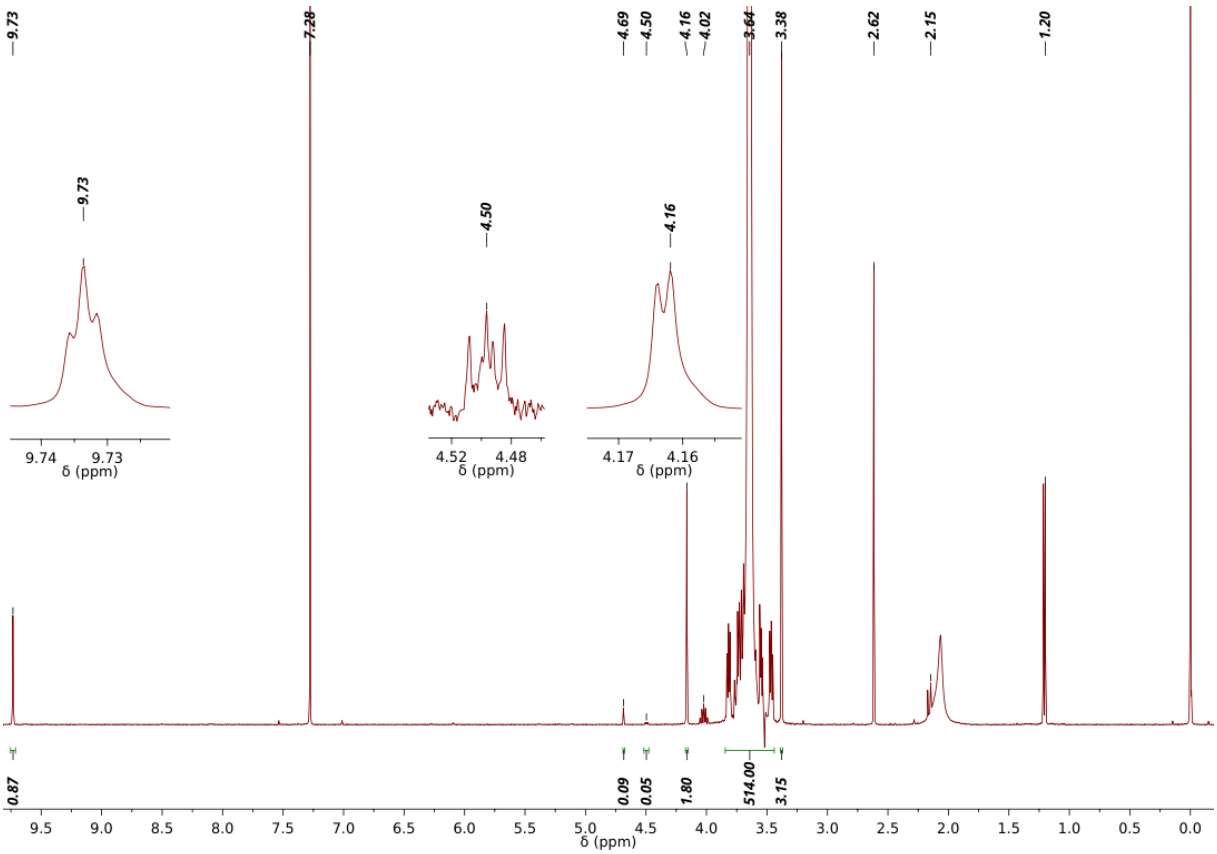

Figure S3. ^{1}H-NMR spectrum of a mPEG5K-ald

Analytical data ^{1}H-NMR, (400 MHz, $CDCl_3$) of mPEG5K-ald.

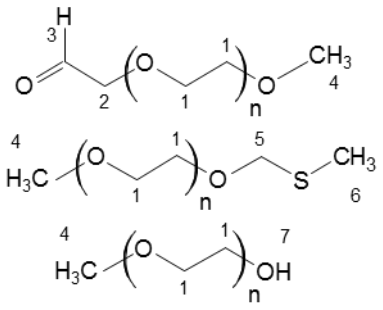

Proton		δ (ppm)	J (Hz)
H_1	s	3.64	
H_2	d	4.16	0.8
H_3	t	9.73	0.8
H_4	s	3.38	
H_5	s	4.69	
H_6	s	2.15	
H_7	t	4.50	
DMSO	s	2.62	

In analyzing the spectrum of mPEG5K-ald, we can identify the resulting peak H1 from the PEG units at 3.64 ppm. By integration of this peak as reference, it makes possible to estimate the yield of the oxidation . The triplet at 9.73 ppm is attributed to H3 from the aldehyde group. The integration of this proton give 0.87 while that of the H2 give 1.8. The yield of the oxidation reaction is therefore about 90%. It can also be noticed the good coherence between the integration of H1 peaks fixed at 514 and that of H4 of the methoxy group termination, which gives about 3 protons. The peaks at 4.69 and 2.15 ppm attest the presence of methylthiomethylether coming from the reaction with the activated DMSO, which represents about 5% of all the mPEG chains. The remaining 5% can be found with the integration of the small multiplet at 4.50 ppm that can be attributed to H7. The proton from hydroxyl

cannot be observed in D_2O due to the fast exchange with D but can be observed in other aprotic organic solvents [11].

3. Additional characterization of DF-SiO_2NPS-PEG5K samples.

3.1 TGA analysis.

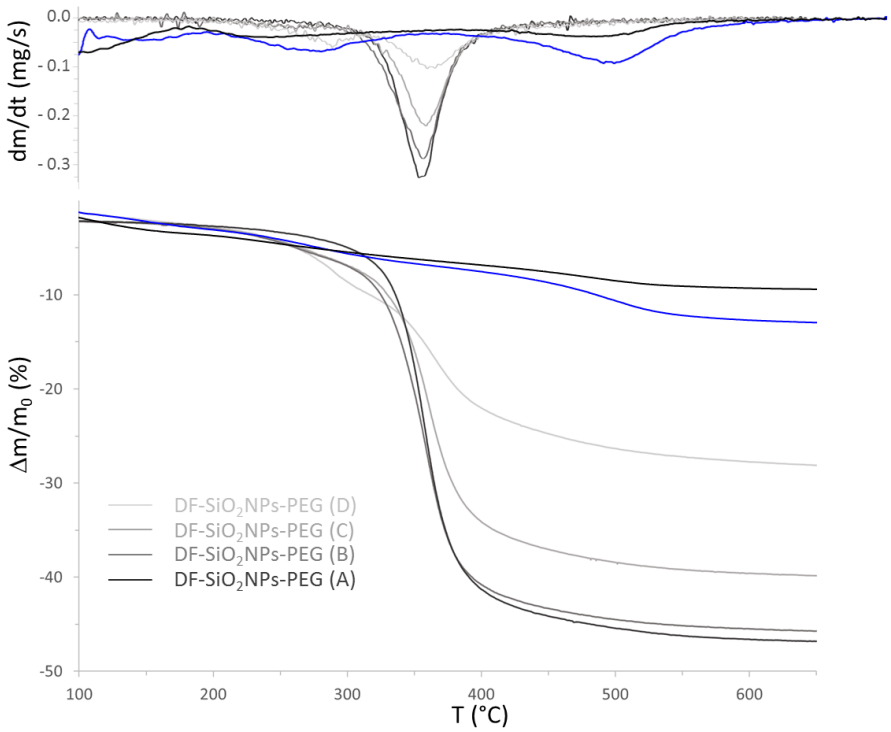

Figure S4. TGA diagrams showing the percentual mass loss of silica nanoparticles (black curve), EDPS-modified silica NPs (blue curve) and diagrams resulting from different levels of PEGylation; up, corresponding differentiated TGA diagrams.

3.2 Grafting density calculations.

		ATG/Ar	ATG/O_2				
Sample	**m_1(300°C)**	**m_2(690°C)**	***% corr***	**m_2^{corr}**	**Δm**	**$\Sigma m_{(EDPS/H_2O)}$**	**$\Delta m_{(PEG)}$**
A	10.1521	5.6465	4.52	5.3913	4.7608	0.3719	4.3889
B	10.4621	6.0325	4.46	5.7635	4.6986	0.3980	4.3002
C	9.9214	6.3675	4.22	6.0988	3.8226	0.4208	3.4018
D	11.8248	9.1210	3.87	8.7680	3.0568	0.6051	2.4517

Table S1. Mass losses values for samples A-D for both thermal cycles under Ar and O_2 and contributions of the polysiloxane film and chemisorbed water. All the masses are expressed in mg.

- *% corr* is a correction factor applied to take into account the additional mass losses during the second thermal cycle under O_2 flux:

$$\%\ corr = \Delta m/m_{2(690°C/O_2)}, \text{ where } \Delta m = m_{1(200°C/O_2)} - m_{2(690°C/O_2)};$$

- $\Sigma m_{(EDPS/H2O)}$: From a given mass of silica NP m_2^{corr} the contribution of propylaminoethylamine moieties and chemisorbed water from silanols of the silica matrix and polysiloxane film are extracted according to the developed surface area.

$$\Sigma m_{(EDPS/H2O)} = S \cdot (d_{(EDPS)} \cdot M_{(C_5H_{13}N_2)} + d_{(H_2O)} \cdot M_{(H_2O)})$$

where, $d_{(EDPS)}$ = 3.40 µmol/m^2, $d_{(H_2O)}$ = 3.93 µmol/m^2 deduced from TGA measurements of DF-SiO_2 NPs-EDPS and DF-SiO_2 NPs, respectively; $M_{(C_5H_{13}N_2)}$ = 101 g/mol and $M_{(H_2O)}$ = 18 g/mol.

- $\Delta m_{(PEG)}$ is the mass of PEG macromolecules for a given sample deduced from the contributions of water and polysiloxane film:

$$\Delta m_{(PEG)} = \Delta m - \Sigma m_{(EDPS/H_2O)}$$

$$\text{with, } \Delta m = m_{1(300°C/Ar)} - m_2^{corr}$$

$$\text{and, } m_2^{corr} = m_{2(690°C/Ar)} - m_{2(690°C/Ar)} \cdot \% \, corr$$

Sample	m_2^{corr}	S (m^2)	$\Delta m_{(PEG)}$ (mg)	σ (µmol/m^2)	σ (molecules/nm^2)
A	5.3913	0.898	4.3889	0.85	0.51
B	5.7635	0.961	4.3002	0.78	0.47
C	6.0988	1.016	3.4018	0.58	0.35
D	8.7680	1.461	2.4517	0.29	0.18

Table S2. Surface grafting density values for each samples.

- S: is the surface developed by the given amount of SiO2 NPs. This value can be deduced by multiplying the mass of calcinated silica by the specific surface area developed by SiO_2 cores of 19 nm (S_{sp} = 166.67 m^2/g):

$$S = m_2^{corr} \cdot S_{sp}$$

- The grafting density, σ, can thus be deduced:

$$\sigma \, (\mu mol/m^2) = \frac{\mathbf{\Delta m(PEG)}}{M_{PEG} \, \mathbf{S}}, \text{ with } M_{PEG} = 5738 \text{ g/mol}, \Delta m_{(PEG)} \text{ in g and S in m}^2$$

$$\text{and } \sigma \, (\mu mol/nm^2) = \frac{\mathbf{\Delta m(PEG)} \times N_A}{M_{PEG} \, \mathbf{S}}, \; N_A \text{ the Avogadro number}, \Delta m_{(PEG)} \text{ in g and S in nm}^2$$

3.2 DLS in PBS and water.

	DLS in PBS		DLS in water	
Sample	Z-Ave(nm)	PDI	Z-Ave(nm)	PDI
DF-SiO2NPs-PEG (A)	50.3	0.13	50.1	0.22
DF-SiO2NPs-PEG (B)	48.8	0.16	49.5	0.17
DF-SiO2NPs-PEG (C)	45.1	0.10	43.0	0.18
DF-SiO2NPs-PEG (D)	45.2	0.19	45.5	0.28

Table S3. Hydrodynamic values and polydispersity index of each samples measured in PBS and ultrapure water by DLS.

References

1. S. Cousinié, M. Gressier, C. Reber, J. Dexpert-Ghys, M.J. Menu, Europium(III) Complexes Containing Organosilyldipyridine Ligands Grafted on Silica Nanoparticles, *Langmuir* 24 (2008) 6208–6214.

2. L. T. Arenas, J. C. P. Vaghetti, C. C. Moro, E. C. Lima, E. V. Benvenutti, T. M. H. Costa, Dabco/silica sol–gel hybrid material. The influence of the morphology on the CdCl2 adsorption capacity, Materials Letters 58 (2004) 895–898.

3. F. A. Pavan, T. M. H. Costa, E. V. Benvenutti, Adsorption of CoCl2, ZnCl2 and CdCl2 on aniline/silica hybrid material obtained by sol–gel method, Colloids Surf., A 226 (2003) 95–100.

4. J. R. Martínez, F. Ruiz, Y. V. Vorobiev, F. Pérez-Robles, J. González-Hernández, Infrared spectroscopy analysis of the local atomic structure in silica prepared by sol-gel, J. Chem. Phys. 109 (1998) 7511–7514.

5. P. Innocenzi, Infrared spectroscopy of sol–gel derived silica-based films: a spectra-microstructure overview, J. Non-Cryst. Solids 316 (2003) 309–319.

6. T. A. Guiton, C. G. Pantano, Infrared reflectance spectroscopy of porous silicas, Colloids Surf. A 74 (1993) 33–46.

7. The Chemistry of Silica; Iler, R. K., Iler, R. K., Eds.; Wiley: New York, 1979; p 98.

8. T. Bayer, K. J. Eichhorn, K. Grundke, H. J. Jacobasch, FTIR spectroscopic studies of interfacial reactions between amino functionalized silicon surfaces and molten maleic anhydride copolymers, Macromol. Chem. Phys. 200 (1999) 852-857.

9. C. H. Chiang, H. Ishida, J. L. Koening, The structure of γ-aminopropyltriethoxysilane on glass surfaces, J. Colloid Interface Sci. 74 (1980) 396.

10. Chemically Modified Surfaces; Vrancken, K. C., Van Der Voort, P., Possemiers, K., Grobet, P., Vansant, E. F., Peseck, J. J., Eds.; Royal Society of Chemistry: Cambridge, U.K., 1994; p 46.

11. J. M. Dust, Z.-H. Fang, and J. M. Harris, Proton NMR Characterization of Poly(ethy1ene glycols) and Derivatives, Macromolecules 23 (1990) 3742-3746.